Int. J. Solids Structures Vol. 21, No. 8, pp. 889–906, 1985
Printed in Great Britain.

0020-7683/85 $3.00 + .00
Pergamon Press Ltd.

A METHOD FOR THE ANALYSIS OF THE TANGENTIAL STRESSES AND THE WEAR DISTRIBUTION BETWEEN TWO ELASTIC BODIES OF REVOLUTION IN ROLLING CONTACT

KLAUS KNOTHE and HUNG LE-THE
Institut für Luft- und Raumfahrt, Technische Universität Berlin, Salzufer 17-19, D-1000 Berlin 10, F.R. Germany

(*Received* 23 *January* 1984; *in revised form* 25 *September* 1984)

Abstract—This study presents a numerical method for computing the tangential stress distribution in the nonelliptical contact area due to creepages during the rolling of two elastic bodies of revolution. The difference is demonstrated between the linear case, when no slip occurs in the whole contact area, and the nonlinear case, when slip occurs in parts of the contact area. The nonlinear case is easily solved by the modification of Kalker's simplified nonlinear theory once the results of the linear case are available. To solve the resulting integral equation for the linear case numerically, the contact area is divided into strips. The tangential stress in each strip can be approximated by second-degree polynomials. The necessary relations for the unknown stress amplitudes are obtained by satisfying the nonslip conditions in two collocation points. The results of the method are compared with those obtained by Kalker for elliptical contact areas.

To illustrate the efficiency of this method, the problem of rolling contact for wheel and rail of railway vehicles, in which a nonelliptical contact area is formed, has been solved. Due to slip in parts of the contact area, the wear mechanisms lead to a change of wheel-rail profiles. For the combination of the new wheel profile ORE S 1002 with the new rail profile UIC 60, the wear rate distribution on a rail profile is demonstrated.

1. INTRODUCTION

The calculation of the tangential forces transmitted between two elastic bodies of revolution in rolling contact is important in many technical areas, e.g. when investigating the stability behaviour of high-speed railway vehicles on track or analysing roller bearings.

It is usually assumed that the surfaces of the two contacting bodies near the contact point may be represented by second degree polynomials, so that the contact area and the normal traction distribution can be calculated by Hertz's theory[1], and the tangential traction distribution due to friction by Kalker's theory. In practise, however this assumption is often not fulfilled. For instance, in the case of contact between a wheel and rail, the contact area becomes considerably nonelliptical due to a possibly abrupt variation of the radii of curvature of the wheel and rail profile near the contact point. The assumption is, however, usually sufficient in the field of railway vehicle dynamics, where only the resultant forces acting on the wheelset are of interest. When the wear of the wheel and rail profile is taken into account, a precise treatment of distribution of tangential stresses in the real contact area is required. The wear due to slip in parts of the contact area leads to a change of geometry of wheel and rail profile, which in turn influences the behaviour of motion of the railway vehicle. Before treating the tangential contact problem between wheel and rail, the classification of this problem in the field of railway vehicle dynamics (short-term behaviour) and in the determination of wear (long-term behaviour) is explained in Fig. 1. The investigation of railway vehicle dynamics using a numerical integration procedure gives the continuous lines.

The investigation of the wearing of profiles is denoted by dashed lines.

A distinction is made between the level of system dynamics describing the behaviour of motion of railway vehicles and the level of contact mechanics.

Let us consider the level of dynamics. We start with the generalized equations of the system (step 1 in Fig. 1). These equations consist of two parts: First, the differential equations of motion, and secondly the constraint conditions between wheel and rail

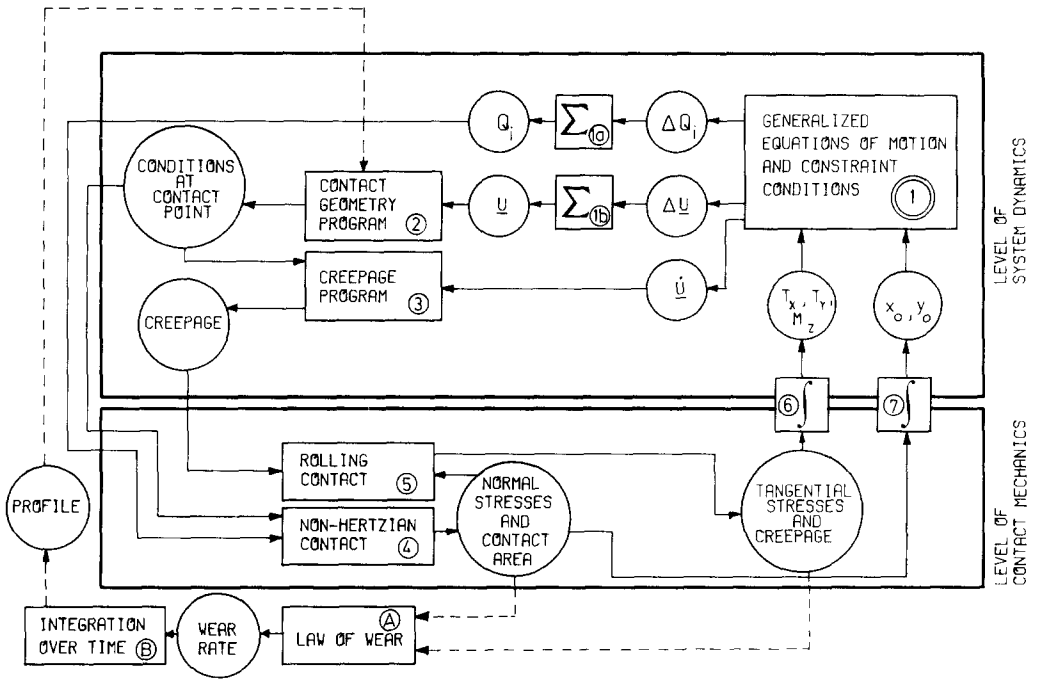

Fig. 1. Contact problem in the field of railway vehicle dynamics.

must be fulfilled. After each step of the simulation, one obtains information about the change of state of displacement $\Delta \underline{u}$ and the change of normal forces ΔQ_i at the contact points. These are added to the displacement vector $\underline{u}$ and the normal forces Q_i (step 1a). Besides the displacement, the velocities of all components of the vehicle are known. In the new position, the constraint condition will no longer be fulfilled. Therefore, in step 2, a contact geometry program[2] is used to check if the profiles are overlapping and to determine the new contact points. In Step 3, the creepages at the contact points must be determined.

Now we come to the level of contact mechanics. If, for a given profile combination the position of a contact point and the applied normal force are known, the contact area, the distribution of normal stresses, and the deformation of profile can be determined (step 4). In the case of Hertzian contact, the results are available in tabular form (see Kalker[3]). In step 5, the tangential stresses arising in the contact area are determined for the given creepages at the contact points and the known distribution of normal stress in the contact area. Integrating the tangential stresses over the contact area (step 6) gives the resultant tangential forces which, in the next integration step, enter into the differential equations of motion described at the level of system dynamics. In Fig. 1, there are two further subordinated feedback loops between the level of contact mechanics and the level of system dynamics. By integration of the normal stresses over the contact area, one again obtains the resultant normal force. However, the application point of the result normal force varies. The very small deviations Δx_0 and Δy_0 can be taken into account in the next integration step (step 7). One could also take profile deformation resulting from normal stresses into consideration. This would have to be done in the geometry program.

Now let us consider the problem of wear, i.e. the long-term behaviour denoted by dashed lines in Fig. 1. Here the wear rate of the wheel and rail profile is determined as a function of creepages and tangential stresses (step A).

Because the wear problem is a long-term process, it is not necessary to calculate the wear rate in each integration step. The wear rate leads to changes in the wheel and rail profiles (step B), which must be taken into consideration in the geometry program and in the treatment of the contact problem. These changes result in a modified running behaviour of the railway vehicle. Thus the long-term feedback loop is closed.

In the present study, a numerical method is developed to determine the tangential

stresses due to creepages in the nonelliptical contact area. The wear rate during hunting motion of the wheelset on track is calculated. The wear rate is determined with regard to elliptical and nonelliptical contact areas to see whether there are relevant differences between both cases or not. The first analysis of the rolling contact problem between wheel and rail was carried out by Carter[4] in 1926. He treated the two-dimensional problem of two cylinders rolling together with longitudinal creepages. Later, Poritzky[5], Fromm[6], Föppl[7], and Buffler[8] investigated the same problems. in 1967 Heinrich and Desoyer[9] extended the investigation to rolling contact of a cylinder rolling on a half space with longitudinal and lateral creepages. The three-dimensional rolling contact problem was first examined by Johnson[10] and Haines and Ollerton[11]. They found the solutions for rolling contact between a sphere and a plane under the action of tangential forces. Kalker[12] generalized the three-dimensional rolling contact problem of two elastic bodies for combinations of longitudinal, lateral, and spin creepage.

Nearly all analyses of this rolling contact problem begin by assuming that the contact area and the normal stress distribution are in accordance with the solution given by Hertz. In 1982, Kalker[13] extended his theory of rolling contact between arbitrary bodies for the case where the shape of contact area is nonelliptical. In order to get an approximate solution, the contact area is divided into rectangular elements.

In our work, the nonelliptical contact area is divided into strips. In the nonlinear case of rolling contact, where slip and adhesion may occur in the contact area, the tangential stresses can be relatively easily determined by modifying Kalker's simplified nonlinear theory. However, the results of the linear rolling contact problem must be known in advance. For the linear rolling contact, in which no slip occurs over the entire contact area, a numerical method is developed to determine tangential forces and the so-called coefficients of creepage.

2. TANGENTIAL CONTACT PROBLEM

2.1 *Basic equations*

Assuming that the two elastic bodies are made of the same material, the normal contact problem and the tangential contact problem can be treated independently. In this case, the tangential displacements are not influenced by the normal stresses nor are the vertical displacements by the tangential stresses.

In the normal contact problem, the two elastic bodies with surfaces S_1 and S_2 are brought into contact at point 0 (see Fig. 2). A cartesian coordinate system is introduced with the contact point as the origin. Axes (x, y) lie in the common tangent plane of the two surfaces at the contact point, with z directed towards body 1. Under the action of the normal force Q, a nonelliptical contact area Ω will replace the contact point 0 of the unloaded state. Assuming that the contact problem between wheel and rail is one of two bodies of revolution with their axes in the same plane, the contact area and the normal pressure transmitted across it are calculated by an approximative method, in which the contact area is divided into strips for the discretization of the resulting Fredholm integral equation of the first kind[14, 15]. When the two elastic bodies are in motion, tangential forces which depend on a relative velocity of the two contacting bodies may be transmitted across the contact area.

2.1.1 *Kinematic relations.* Consider the two rolling elastic bodies (see Fig. 3), we denote by $\underline{v}_{r1}(\underline{v}_{r2})$ the velocity of the upper (lower) body. If we disregard the elastic tangential deformation, then according to Kalker the relative velocity at a contact point (x, y) is given by the relation

$$\underline{v}_{r1} - \underline{v}_{r2} = v_m\{\nu_x - \phi y;\ \nu_y + \phi x\}, \tag{1}$$

where ν_x, ν_y, ϕ are the longitudinal creepage, the lateral creepage, and the spin creepage. The mean rolling velocity v_m is defined by

$$\tfrac{1}{2}(\underline{v}_{r1} + \underline{v}_{r2}) = \{-v_m;\ 0\}. \tag{2}$$

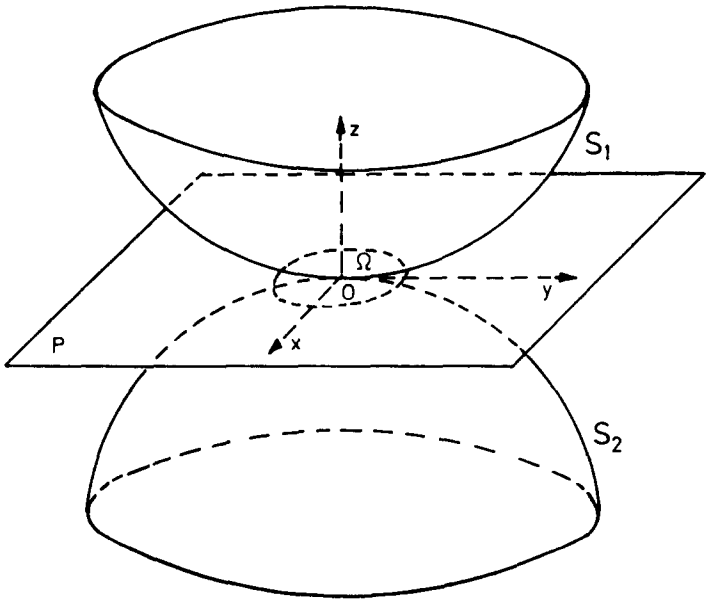

Fig. 2. Two contacting bodies in undeformed state (contact point 0) and in deformed state (contact area Ω).

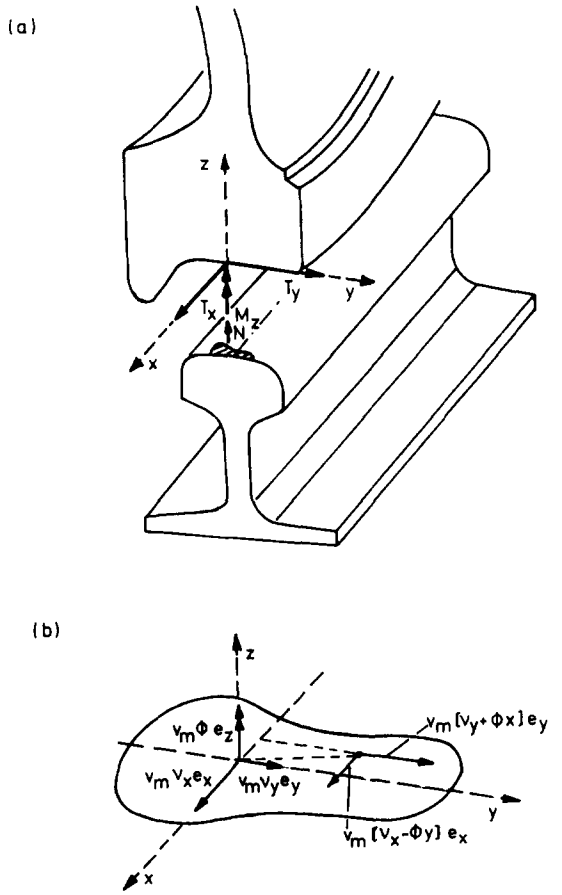

Fig. 3. Forces and moment applied to wheel set and rail (a), creepages in contact area (b).

Taking into account elastic displacements in the contact area, the real relative velocity of the bodies in the contact range is given by

$$\underline{v}_1 - \underline{v}_2 \equiv \{v_x; v_y\} = v_m \left\{ v_x - \phi y + \frac{\partial u_x}{\partial x} - \frac{1}{v_m}\frac{\partial u_x}{\partial t} ; v_y + \phi x + \frac{\partial u_y}{\partial x} - \frac{1}{v_m}\frac{\partial u_y}{\partial t} \right\}, \tag{3}$$

where the difference of the elastic displacements is defined by

$$u_x = u_{x1} - u_{x2}, \qquad u_y = u_{y1} - u_{y2}.$$

Under conditions of steady rolling, the time derivatives $\partial u_x/\partial t$, $\partial u_y/\partial t$ of the elastic displacements vanish. Dividing the real relative velocity by the mean rolling velocity, v_m, the relative slip of a particle of the upper body with respect to a particle of the lower body is defined by

$$\underline{s} \equiv \frac{\underline{v}_1 - \underline{v}_2}{v_m} = \left\{ v_x - \phi y + \frac{\partial u_x}{\partial x} ; v_y + \phi x + \frac{\partial u_y}{\partial x} \right\}. \tag{4}$$

2.1.2. *Constitutive relations.* In accordance with Love[16], the elastic displacements u_x, u_y, u_z at the boundary of the elastic half-space acted on by the stresses X, Y, Z, are given by the Boussinesq-Cerrutti's equations, see Fig. 4.

$$\begin{bmatrix} u_x(x, y) \\ u_y(x, y) \\ u_z(x, y) \end{bmatrix} = \frac{1}{\pi G} \int_\Omega \begin{bmatrix} h_{11} & h_{12} & h_{13} \\ h_{21} & h_{22} & h_{23} \\ h_{31} & h_{32} & h_{33} \end{bmatrix} \begin{bmatrix} X(x^*, y^*) \\ Y(x^*, y^*) \\ Z(x^*, y^*) \end{bmatrix} dx^*\, dy^* \tag{5}$$

where

$$h_{11} = \frac{1 - \sigma}{R} + \frac{\sigma(x - x^*)}{R^3}; \qquad h_{12} = \frac{\sigma(x - x^*)(y - y^*)}{R^3}$$

$$h_{22} = \frac{1 - \sigma}{R} + \frac{\sigma(y - y^*)^2}{R^3}; \qquad h_{13} = \frac{\kappa(x - x^*)}{R^2}; \qquad h_{23} = \frac{\kappa(y - y^*)}{R^2}$$

$$h_{33} = \frac{1 - \sigma}{R}; \qquad h_{jk} = h_{kj}\ (j \neq k)$$

$$\frac{1}{G} = \frac{1}{2}\left(\frac{1}{G_1} + \frac{1}{G_2}\right); \qquad \kappa = G\left(\frac{1 - 2\sigma_1}{4G_1} - \frac{1 - 2\sigma_2}{4G_2}\right)$$

$$\frac{\sigma}{G} = \frac{1}{2}\left(\frac{\sigma_1}{G_1} + \frac{\sigma_2}{G_2}\right); \qquad R = [(x - x^*)^2 + (y - y^*)^2]^{1/2}.$$

$G_1(G_2)$ is the shear modulus of the upper (lower) body and σ_1 (σ_2) is Poisson's ratio

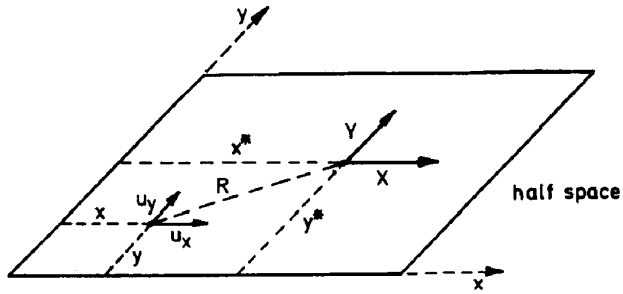

Fig. 4. Exact theory (half space theory).

of the upper (lower) body. When the two bodies are made of the same material, i.e. $\sigma_1 = \sigma_2$, $G_1 = G_2$, or when they are incompressible, i.e. $\sigma_1 = \sigma_2 = 0.5$, the constant κ vanishes. In these cases, the assumption that neither the tangential displacements u_x, u_y are influenced by the normal stress Z nor the normal displacement u_z by the tangential stresses X, Y is fulfilled.

We will now deal with the transmission of force during the rolling of two bodies made of the same material, so that the tangential displacements u_x, u_y are given by

$$u_x(x, y) = \frac{1}{\pi G} \int \{h_{11} \cdot X(x^*, y^*) + h_{12} \cdot Y(x^*, y^*)\} \, dx^* \, dy^* \tag{6a}$$

$$u_y(x, y) = \frac{1}{\pi G} \int \{h_{12} \cdot X(x^*, y^*) + h_{22} \cdot Y(x^*, y^*)\} \, dx^* \, dy^*. \tag{6b}$$

When using the exact relations (4a,b) to determine the tangential force transmitted in the contact area we speak of Kalker's exact theory.

In order to reduce the computing times, Kalker developed the simplified theory, in which the constitutive relations based on Winkler's model are chosen as

$$u_x = L_x X; \qquad u_y = L_y Y. \tag{7}$$

In this model, the corresponding points of the bodies in contact are continuously connected by springs. This can be modelled as the thin elastic layers on a completely rigid body.

2.1.3. *Slip and adhesion condition.* To calculate the tangential stresses X and Y, the adhesion and slip conditions must be satisfied. The contact area is divided into the adhesion and slip area (see Fig. 5). In the adhesion area, there is no slip between the contacting points. Denoting the normal stress by Z, the coefficient of the friction by μ, the adhesion condition is

$$\sqrt{X^2 + Y^2} < \mu Z; \qquad \{s_x; s_y\} = \{0; 0\}. \tag{8a,b}$$

In the slip area it is necessary that

$$\sqrt{X^2 + Y^2} < \mu Z; \qquad s_x/s_y = X/Y. \tag{9a,b}$$

2.1.4. *Determination of the tangential stresses.* In the exact theory, the constitutive relationships (6a,b) are substituted into the kinematic relation (3). In the linear case, in which the adhesion occurs over the whole contact area (except a very narrow strip at the trailing edge), then both equations are obtained by means of eqns (8a,b)

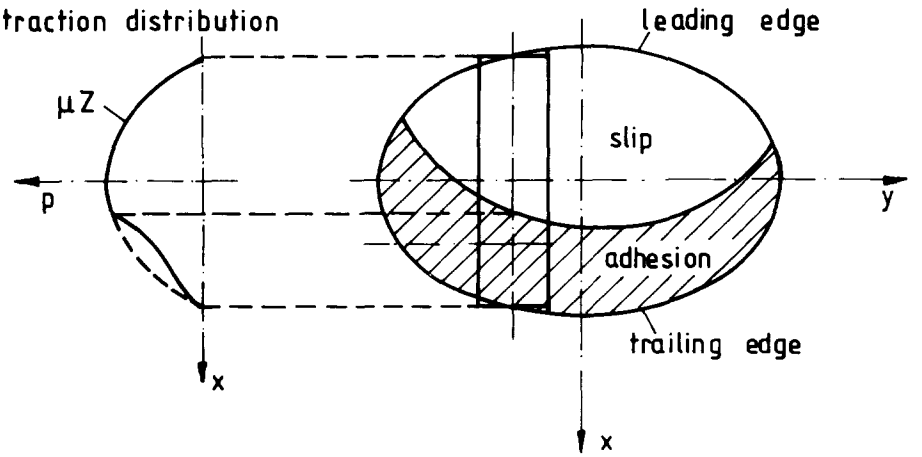

Fig. 5. Adhesion and slip in contact area and corresponding conditions.

$$s_x \equiv 0 = v_x - \phi y + \frac{1}{G\pi}\int_\Omega \{g_{11}\cdot X(x^*, y^*) + g_{12}\cdot Y(x^*, y^*)\}\, dx^*\, dy^* \quad (10a)$$

$$s_y \equiv 0 = v_y + \phi x + \frac{1}{G\pi}\int_\Omega \{g_{12}\cdot X(x^*, y^*) + g_{22}\cdot Y(x^*, y^*)\}\, dx^*\, dy^* \quad (10b)$$

where

$$g_{11} \equiv \frac{\partial h_{11}}{\partial x} = \frac{(3\sigma - 1)(x - x^*)}{R^3} - \frac{3\sigma(x - x^*)^3}{R^5}$$

$$g_{12} \equiv \frac{\partial h_{12}}{\partial x} = \frac{\sigma(y - y^*)}{R^3} + \frac{3\sigma(x - x^*)^2(y - y^*)}{R^5}$$

$$g_{22} \equiv \frac{\partial h_{22}}{\partial x} = \frac{(\sigma - 1)(x - x^*)}{R^3} - \frac{\sigma(x - x^*)(y - y^*)^2}{R^5}.$$

The integral equations (10a,b) have singular kernels. We shall see later that, for the approximate functions introduced, Cauchy's principal values always exist.

When the contact area is divided into an adhesion zone and a slip zone, then the analysis becomes more complicated, see Kalker[3, 12]. In this case, for the calculation of the tangential stresses, the two integro-differential equations are obtained. This nonlinear tangential contact problem was numerically solved by Kalker for the elliptical contact area[12] and the nonelliptical contact area[13].

Using the simplified theory in the case of pure adhesion in the whole contact area, one obtains two ordinary differential equations for the tangential stresses

$$s_x \equiv v_x - \phi y + L_x \frac{\partial X}{\partial x} = 0;\ s_y \equiv v_y + \phi x + L_y \frac{\partial Y}{\partial y} = 0. \quad (11a,b)$$

The simplified theory has to conform to the exact theory. Therefore, not only the two flexibilities L_x, L_y, but four fictive flexibilities L_1 to L_4 are introduced, as by Kalker[18]:

$$w_x \equiv v_x/L_1 - \phi y/L_4 + \partial X/\partial x = 0 \quad (12a)$$

$$w_y \equiv v_y/L_2 + \phi x/L_3 + \partial Y/\partial x = 0. \quad (12b)$$

In the linear case, the tangential stresses X, Y are calculated by the integration of eqns (12a,b). In the nonlinear case, they are determined according to Kalker[17, 18] by means of a numerical method described in Section 3.2.1.

By treating the nonlinear tangential contact problem based on the simplified theory, the main difficulty is that the fictive flexibilities L_1 to L_4 are not known. They must be chosen such that, for the linear case, the tangential forces of the simplified theory coincide with those of the exact theory. Therefore, it is necessary to solve the exact linear tangential contact problem for nonelliptical contact areas.

2.2. *Exact linear determination of the tangential stresses for nonelliptical contact areas*

2.2.1. *Approximate solution of the integral equation.* To solve the integral equations (10a,b) the contact area is divided into M strips parallel to the rolling direction. In each strip, the tangential stresses X_i, Y_i are approximated by quadratic polynomials in the x-direction, which vanish at the leading edge (see Fig. 6)

$$X_i \equiv \hat{X}_{Li}(1 - x_i/x_{ri}) + \hat{X}_{Qi}(1 - x_i^2/x_{ri}^2) = \hat{X}_{Li} f_{Li} + \hat{X}_{Qi} f_{Qi} \quad (13a)$$

$$Y_i \equiv \hat{Y}_{Li}(1 - x_i/x_{ri}) + \hat{Y}_{Qi}(1 - x_i^2/x_{ri}^2) = \hat{Y}_{Li} f_{Li} + \hat{Y}_{Qi} f_{Qi} \quad (13b)$$

$$i = 1, \ldots, M.$$

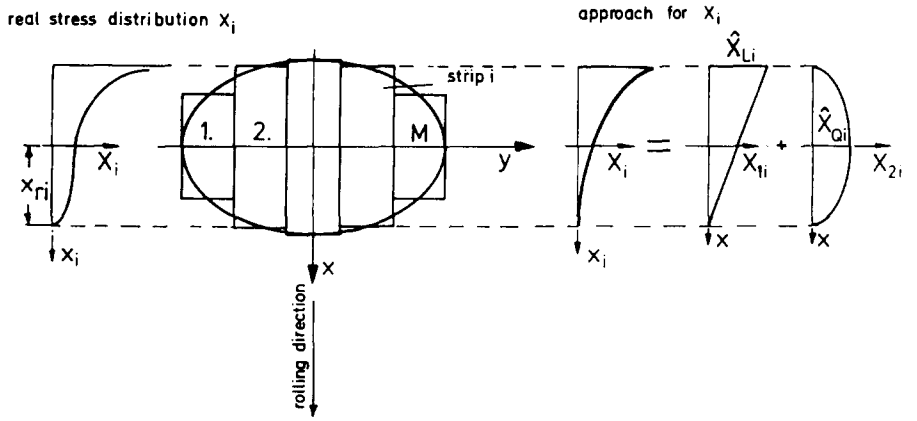

Fig. 6. Approach function for the tangential stresses.

Here the strip length is denoted by $2x_{ri}$ and the stress amplitudes by $\hat{X}_{Li}$, $\hat{X}_{Qi}$, $\hat{Y}_{Li}$, $\hat{Y}_{Qi}$.

Introducing the approximate functions (13a,b) into both integral equations (10a,b), two algebraic equations in terms of $4M$ unknown stress amplitudes are obtained

$$s_x \equiv v_x - \phi y + \frac{1}{\pi G}\sum_{i=1}^{M}\int_{\Omega_i}\{h_{11}\cdot[\hat{X}_{Li}f_{Li} + \hat{X}_{Qi}f_{Qi}] + h_{12}\cdot[\hat{Y}_{Li}f_{Li} + \hat{Y}_{Qi}f_{Qi}]\}\,\mathrm{d}\Omega_i = 0 \tag{14a}$$

$$s_y \equiv v_y + \phi x + \frac{1}{\pi G}\sum_{i=1}^{M}\int_{\Omega_i}\{h_{12}\cdot[\hat{X}_{Li}f_{Li} + \hat{X}_{Qi}f_{Qi}] + h_{22}\cdot[\hat{Y}_{Li}f_{Li} + \hat{Y}_{Qi}f_{Qi}]\,\mathrm{d}\Omega_i = 0. \tag{14b}$$

The resulting integrals can be solved analytically, see Le The[19]. The Cauchy's principal values of the singular integrals exist.

Because the eqns (14a,b) are satisfied at $2M$ points of the contact area—the so-called collocation points—we can obtain $4M$ equations for $4M$ unknown stress amplitudes,

$$\frac{1}{\pi G}\sum_{i=1}^{M}\begin{bmatrix} K_{11} & K_{12} & K_{13} & K_{14} \\ K_{21} & K_{22} & K_{23} & K_{24} \\ K_{31} & K_{32} & K_{33} & K_{34} \\ K_{41} & K_{42} & K_{43} & K_{44} \end{bmatrix}_i \begin{Bmatrix} \hat{X}_L \\ \hat{X}_Q \\ \hat{Y}_L \\ \hat{Y}_Q \end{Bmatrix}_i = \begin{Bmatrix} -v_x + \phi y_1 \\ -v_y - \phi x_1 \\ -v_x + \phi y_2 \\ -v_y - \phi x_2 \end{Bmatrix}_j \qquad j = 1, \ldots, M. \tag{15}$$

If one introduces the following abbreviations

$$\underline{h}_j^T \equiv \{h_1; h_2; h_3; h_4\}_j^T = \{-v_x + \phi y_1; -v_y - \phi x_1; -v_y + \phi y_2; -v_y - \phi x_2\}_j^T$$
$$\mathbf{h}^T \equiv \{\mathbf{h}_1^T, \mathbf{h}_2^T \ldots \mathbf{h}_M^T\}; \quad \hat{\mathbf{X}}_i^T = \{\hat{X}_L; \hat{X}_Q; \hat{Y}_L; \hat{Y}_Q\}_i^T \tag{16}$$

and uses matrices, then the eqns (14a,b) can be rewritten

$$\frac{1}{\pi G}\mathbf{K}\hat{\mathbf{X}} = \mathbf{h}. \tag{17}$$

The vector $\mathbf{h}$ is defined for a given position of the collocation points. Inverting the eqn (17), one gets the vector $\hat{\mathbf{X}}$ of the stress amplitudes.

The position of the collocation points must now be determined. An additional difficulty here is the singularity of the tangential stresses at the trailing edge in the linear case, Fig. 7 (see Desoyer and Kalker[9, 20]).

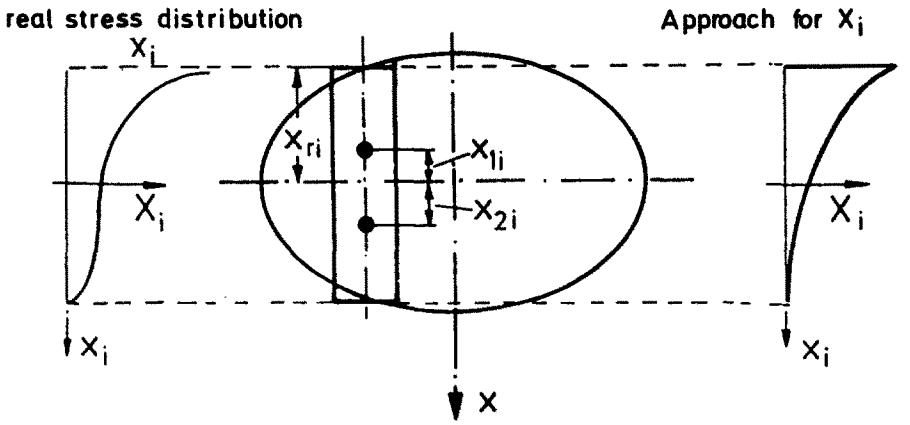

Fig. 7. Collocation points.

In the following, we will consider whether the approximate quadratic functions which are introduced are adequate for at least the tangential forces to be determined accurately enough.

The collocation points are calculated in such a way that the deviation between the tangential forces in the linear case and those obtained by Kalker for an elliptical contact area is minimal. For all axial ratios between 1:10 and 10:1, almost the same values of x_{1i}/x_{ri}, x_{2i}/x_{ri} are obtained (see Table 1). The deviations of the tangential forces and of the coefficient of creepage C_{ik} are below 5% (see Table 2).

Table 1. Depence of values $x_1 = x_{ri}/c_1$ and $x_2 = x_{ri}/c_2$ on ratio of semi-axes of contact ellipse.

	g	c_1	c_2
b>a	0.1	2.474	1.233
	0.2	2.413	1.241
	0.3	2.353	1.249
	0.4	2.317	1.252
	0.5	2.294	1.254
	0.6	2.295	1.257
	0.7	2.278	1.255
	0.8	2.278	1.253
	0.9	2.267	1.250
	1.0	2.259	1.248
b<a	0.9	2.261	1.248
	0.8	2.250	1.245
	0.7	2.253	1.243
	0.6	2.241	1.237
	0.5	2.230	1.234
	0.4	2.210	1.226
	0.3	2.184	1.213
	0.2	2.147	1.199
	0.1	2.196	1.162

g = a/b for b>a
g = b/a for a>b

2.2.2. *Numerical results of the linear determination of the tangential stress.* The collocation points obtained above are now used to determine the tangential forces in the nonelliptical contact area. Thus, the tangential forces or the coefficients of creepage of the exact linear theory are solved. In the special contact cases of the lateral displacements of the wheelset against the rail $\hat{u}_y = 0{,}0$ mm and $\hat{u}_y = 1{,}0$ mm, the creepage coefficients are found in Table 3.

Here it is found that the tangential force T_x depends on the spin ϕ due to the asymmetry of the contact area with respect to the x axes.

$$\begin{Bmatrix} T_x \\ T_y \\ M_z \end{Bmatrix} = \begin{bmatrix} C_{11} & 0 & C_{13} \\ 0 & C_{22} & C_{23} \\ C_{31} & C_{32} & C_{33} \end{bmatrix} \begin{Bmatrix} \nu_x \\ \nu_y \\ \phi \end{Bmatrix}. \tag{18}$$

Table 2. Comparison with Kalker's solution for creepage coefficients ($\sigma_1 = \sigma_2 = 0.25$).

g		Present work			Solution to Kalker		
		c_{11}	c_{22}	c_{23}	c_{11}	c_{22}	c_{23}
b>a	0.1	3.44	2.62	0.47	3.31	2.52	0.47
	0.2	3.49	2.72	0.60	3.37	2.63	0.60
	0.3	3.57	2.84	0.72	3.44	2.75	0.71
	0.4	3.65	2.97	0.83	3.53	2.88	0.82
	0.5	3.74	3.11	0.93	3.62	3.01	0.93
	0.6	3.84	3.24	1.04	3.72	3.14	1.03
	0.7	3.94	3.37	1.15	3.81	3.28	1.14
	0.8	4.04	3.51	1.25	3.91	3.41	1.15
	0.9	4.14	3.64	1.36	4.01	3.54	1.36
	1.0	4.24	3.77	1.47	4.12	3.67	1.47
b<a	0.9	4.35	3.90	1.58	4.22	3.81	1.59
	0.8	4.49	4.08	1.74	4.36	3.99	1.75
	0.7	4.67	4.30	1.93	4.54	4.21	1.95
	0.6	4.90	4.58	2.19	4.78	4.50	2.23
	0.5	5.52	4.96	2.57	5.10	4.90	2.62
	0.4	5.69	5.52	3.15	5.57	5.48	3.24
	0.3	6.43	6.40	4.14	6.34	6.40	4.32
	0.2	7.84	8.07	6.27	7.78	8.14	6.63
	0.1	11.59	12.65	13.42	11.70	12.80	14.60

g = b/a for b<a
g = a/b for b>a

Table 3. Creepage coefficients for nonelliptical contact area.

u_y [mm]	c_{11}	c_{22}	c_{13}	c_{23}
0.0	$4.09\ a_1 b_1$	$3.39\ a_1 b_1$	$13.04\ a_1 b_1$	$1.04\ a_1 b_1^3$
1.0	$7.85\ a_2 b_2$	$6.53\ a_2 b_2$	$-33.44\ a_2 b_2$	$3.02\ a_2 b_2^3$

$a_1 = 4.95$ mm ; $a_2 = 9.39$ mm
$b_1 = 7.14$ mm ; $b_2 = 3.00$ mm

When the following coordinate transformation is introduced

$$x^* = x \qquad (19)$$
$$y^* = y - \bar{y}$$

with

$$\bar{y} = -C_{13}/C_{11},$$

the tangential forces are written in the new coordinate system

$$\begin{bmatrix} T_x \\ T_y \\ M_z \end{bmatrix} = \begin{bmatrix} C_{11}^* & 0 & 0 \\ 0 & C_{22}^* & C_{23}^* \\ 0 & C_{32}^* & C_{33}^* \end{bmatrix} \begin{bmatrix} \nu_x^* \\ \nu_y^* \\ \phi^* \end{bmatrix} \qquad (20)$$

where ν_x^*, ν_y^*, ϕ^* are the rigid-body creepages at the origin O*.

2.3. *Nonlinear determination of the tangential stresses in the simplified theory*

2.3.1. *Adaptation to the exact theory.* When determining the tangential stresses based on the simplified theory the flexibilities L_1 to L_4 of Winkler's model must be determined, which occurs in the following ordinary differential equations

$$w_x \equiv \nu_x/L_1 - y\phi/L_4 + \partial X/\partial x \qquad (21a)$$

$$w_y \equiv \nu_y/L_2 + x\phi/L_3 + \partial Y/\partial x. \qquad (21b)$$

They are determined in such a way that in the linear case (pure adhesion) the tangential forces of the simplified theory coincide with those of the exact theory. In the linear case, the real creepage vanishes, see eqns (11a,b). Integrating the tangential stresses over the contact area the tangential forces are obtained

$$\begin{Bmatrix} T_x^* \\ T_y^* \end{Bmatrix} = \begin{bmatrix} B_{11}L_1 & 0 & B_{13}L_4 \\ 0 & B_{22}L_2 & B_{23}L_3 \end{bmatrix} \begin{Bmatrix} \nu_x \\ \nu_y \\ \phi \end{Bmatrix}. \qquad (22)$$

Adapting these tangential forces to those of the exact theory, eqn (18), we obtain the following expressions for the flexibilities

$$L_1 = C_{11}/B_{11}; \qquad L_2 = C_{22}/B_{22} \qquad (23a)$$

$$L_3 = C_{23}/B_{23}; \qquad L_4 = C_{13}/B_{13}. \qquad (23b)$$

Because the spin moment M_z is unimportant in railway vehicle dynamics, its adaption is unnecessary. However, when investigating wear it must be taken into account. For this, it is assumed as an approximation that the flexibilities L_1 to L_4 obtained above can be used to determine the moment M_z.

2.3.2. *Nonlinear determination of the tangential stresses.* To calculate the tangential stresses in the nonlinear case the differential equations (21a,b) are integrated by means of Kalker's algorithm. Here the contact area is divided into strips. Integrating the differential equations (21a,b) by the integration "step" Δx, one gets the following difference equations for the tangential stresses.

$$\Delta x(\nu_x/L_1 - \phi y/L_4) - X_k + X_{k+1} = w_x \Delta x \qquad (24a)$$

$$\Delta x(\nu_y/L_2 + \phi[x_k - \Delta x/2]/L_4) - Y_k + Y_{k-1} = w_y \Delta x$$

$$k = 0, \ldots, N-1 \text{ and } \Delta x = \frac{2x_r}{N}. \qquad (24b)$$

The adhesion and slip conditions (8,9) must be fulfilled. Details are described by Kalker[18]. The integration begins at the leading edge, where the stresses X_0, Y_0 vanish (see Fig. 5).

3. NUMERICAL RESULTS OF THE TANGENTIAL STRESS CALCULATION

By means of the numerical method developed here, the tangential stresses in nonelliptical contact area and the subdivision of the contact area into the adhesion and slip area were calculated for the rolling contact between the wheel and rail. A profile combination ORE S 1002/UIC 60 was used, with the following parameters being taken as a basis:

$$Q = 60\,000\ [N] \qquad \nu_1 = \nu_2 = 0.277 \qquad E_1 = E_2 = 204320\ [N/\text{mm}^2].$$

With the lateral displacement $u_y = 0.0$ mm of the wheelset against the rail, the contact point was determined by means of Hauschild's procedure[2]. The nonelliptical contact area (replacing the contact point) and the corresponding normal stress distribution were calculated by our method (see Knothe/Le The[14, 15]). The tangential stresses and the subdivision of the nonelliptical contact area into the adhesion and slip area are represented in Fig. 8 for a special creepage combination, and compared with those of the elliptical contact area. The comparison shows that, due to the great deviation of the contact area from the elliptical form and due to the nonellipsoidal normal stress distribution, the slip area deviates greatly from that in the Hertzian contact ellipse.

4. CALCULATING OF WEAR OF WHEEL AND RAIL PROFILES

4.1. *Theory of wear*

Wear is a typical phenomenon during rolling and sliding of two bodies of revolution. Due to slip, the rupture of the surface layers is localized in a small volume of material which is removed from the rubbing zone in the form of wear particles. The physicochemical processes, such as adhesion, abrasion, tribochemical reactions, and delamination which characterize the rupture of the surface layers are generally termed wear mechanisms.

Various scientists have developed wear theories in which the physicomechanical characteristics of the materials and the physical conditions (e.g. the resistance of the rubbing bodies and the stress state in the contact area) are taken into consideration.

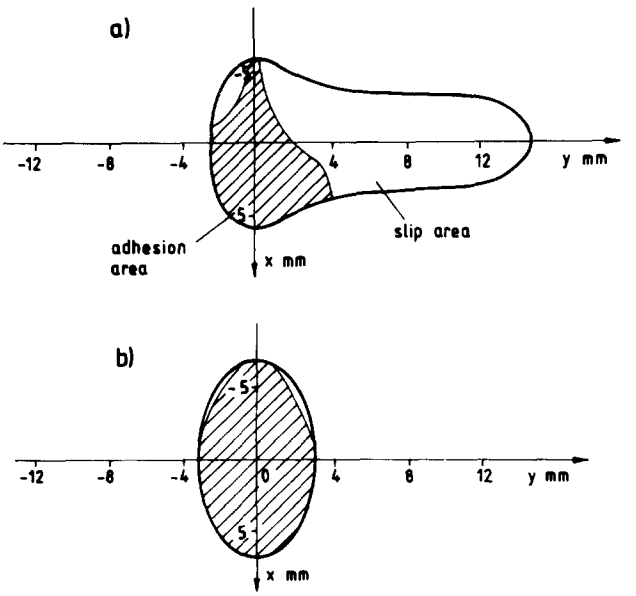

Fig. 8. Subdivision of nonelliptical contact area (a) and of elliptical contact area (b) into adhesion and slip area for a creepage combination: $\nu_x = 0.0$; $\nu_y = 0.0$; $\phi = 0.0005$ 1/m.

Here, some well-known theories are mentioned briefly. In 1940, Holm[21], starting from the atomic mechanism of wear, calculated the volume of substance worn over unit sliding path. Burwell and Strang[22] in 1952, Archard[23] in 1953, and Archard and Hirst[24] in 1956 developed an adhesion theory of wear, and proposed a theoretical equation identical in structure with Holm's equations. In 1957, Kragelski developed the fatigue theory of wear. This theory of wear has been widely accepted by scientists in different countries. Because of the asperities of real bodies, their interaction in sliding is discrete, and contact occurs at individual locations, which, taken together, form the real contact area. Under normal force, the asperities penetrate into each other or are flattened out, and in the region of real contact points corresponding stresses and strains arise. In sliding, a fixed volume of material is subjected to the many times repeated action, which weakens the material and leads finally to rupture (see Kragelsky[25]). In 1973, Fleischer[26] formulated his energy theory of wear. The main concept of this theory is that the separation of wear particles requires that a certain volume of material accumulates a specific, critical store of internal energy. It is known that a large part of the work done in sliding is dissipated as heat, and that small proportion of it accumulates in the material as internal potential energy. When the energy attains a critical value, plastic flow of the material occurs in this volume or a crack is formed. Further theories of wear are found in [25]. Although these theories are based on different wear mechanisms, they give the proportionality relation between the volume of wear W_V and the frictional work W_R

$$W_V = I_W \cdot W_R. \tag{25}$$

The proportionality coefficient I_w is determined by the geometrical and physical properties of rubbing bodies.

4.2. *Basic equations*

The determination of the wear arising in the rolling contact between wheel and rail is based on eqn (25). A wheelset running along the track at constant speed has an additional quasi-sinusoidal motion, as shown in Fig. 9, as a result of which creepages occur in the contact area which induce tangential forces. The frictional power is given

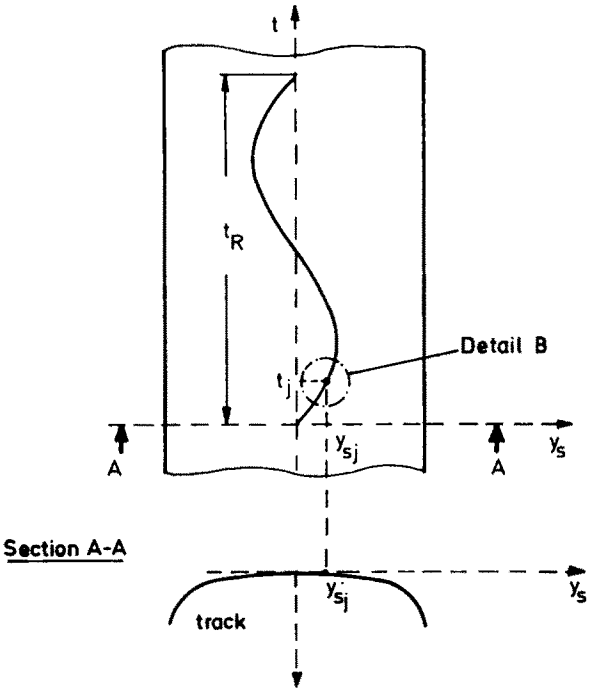

Fig. 9. Quasi-sinusoidal motion of wheelset on track.

by

$$P_R(t) = \int_\Omega (v_x X + v_y Y)\, d\Omega \tag{26}$$

where v_x, v_y are the components of the relative velocity of the contacting particles, and X, Y are the components of the tangential stress acting on those particles. In the simplified nonlinear theory, i.e. by using the relations (4) and (7), the frictional power can be written in the form

$$P_R(t) = v_m \int_\Omega \left[\left(\nu_x - \phi y + L_x \frac{\partial X(x, y)}{\partial x} \right) X(x, y) + \left(\nu_y + \phi x + L_y \frac{\partial Y(x, y)}{\partial x} \right) Y(x, y) \right] d\Omega. \tag{27}$$

By giving a motion state which, of course, depends on the initial existing profile combination and on the bogie configuration, it is possible to calculate the volume of wear as well as to assess the wear sensitivity of different profile combinations of different bogie configurations.

To this end, the wear volume is determined over an interval Δt at time t_j and is distributed over the whole contact area (Fig. 10). If the wheel and rail profile are divided into strips, then the wear volume W^*_{vij} arising in strips of the contact area can be related to strips of the wheel and rail profile. The distribution of wear volume for the wheel and rail profile can then be determined by transferring all the individual distributions at the different points in time t_j. The additional assumption which is necessary, namely that all points on the wheel circumference, and all points on the rail longitudinal display all possible modes of motion equally often, will certainly be fulfilled over time. To carry out the integration in eqn (27), the contact area is divided into M strips, so that

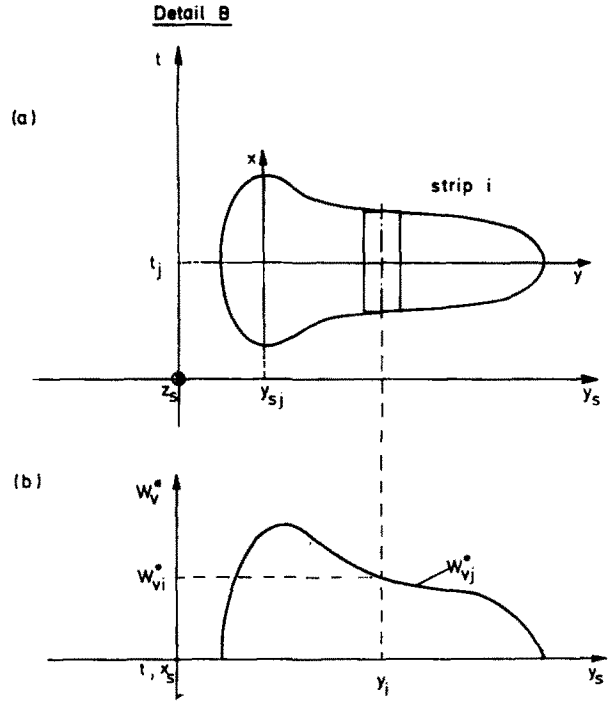

Fig. 10. Contact area at time t_j (a) and distribution of wear rate (b).

we can now write

$$P_R(t) = v_m \sum_{i=1}^{M} \left[\int_{\Omega_i} \{(v_x - \phi y_i)X(x, y_i) + (v_y + \phi x)Y(x, y_i)\} \, dx \, dy + \int_{\Omega_i} \left\{ \frac{\partial X(x, y_i)}{\partial x} X(x, y_i) + \frac{\partial Y(x, y_i)}{\partial x} Y(x, y) \right\} dx \, dy \right]. \quad (28)$$

Taking into consideration the boundary conditions that the tangential stresses at the edges must be equal to zero, the second integral vanishes. The first integral yields

$$P_R(t) = v_m \sum_{i=1}^{M} (T_{xi}v_x + T_{yi}v_y + M_{zi}\phi), \quad (29)$$

i.e. in order to calculate the frictional power, the tangential forces T_{xi}, T_{yi}, and the moment M_{zi} acting in each strip of the contact area, are multiplied by the longitudinal creepage v_x and the lateral creepage v_y and spin creepage ϕ, respectively, then the three resulting parts are added together. Introducing the notation for the frictional power in each strip

$$P^*_{Ri}(t) = v_m(T_{xi}v_x + T_{yi}v_y + M_z\phi), \quad (30)$$

it is found that

$$P_R(t) = \sum_{i=1}^{M} P^*_{Ri}(t). \quad (31)$$

The frictional work is determined by the integration of the frictional power over the rolling time t_R of the wheel on the rail, i.e.

$$W_R = \int_0^{t_R} \sum_{i=1}^{M} P^*_{Ri}(t) \, dt. \quad (32)$$

The numerical integration of eqn (31) with the integration step Δt leads to

$$W_R = \Delta t \sum_{j=1}^{N} \left(\sum_{i=1}^{M} P^*_{Ri} \right)_j, \quad (33)$$

where

$$\Delta t = t_R/(N - 1).$$

The wear volume after the rolling time t_R can now be calculated by

$$W_V = I_w \, \Delta t \sum_{j=1}^{N} \left(\sum_{i=1}^{M} P^*_{Ri} \right)_j. \quad (34)$$

Introducing the following abbreviation

$$W^*_{vi} = I_w P^*_{Ri} \Delta t, \quad (35)$$

eqn (34) can be written in the form

$$W_V = \sum_{j=1}^{N} \sum_{i=1}^{M} W^*_{vij}. \quad (36)$$

The wear volume related to the strip of the contact area W^*_{vij} must now be reduced to that related to the K strips of the wheel or rail profile

$$\sum_{j=1}^{N}\sum_{i=1}^{M} W^*_{ij} = \sum_{k=1}^{K} W_{vk}. \tag{37}$$

To determine the wear rate, i.e. the variation of the profile in unit time, the wear volume related to strip must be divided by the strip width Δy, the rolling time t_R, and the length of track L covered in this time.

4.3. *Numerical results*

In this section, we give the results of our first investigation of the wear of wheel and rail profile. For the wear analysis a new wheel–new rail profile combination 0RE S 1002/UIC 60 was used. The gauge of the track was 1435 mm. A first jump of the contact point occurs at a lateral displacement $u_y \cong 0.2$ mm.

For an exact investigation of the profile development the analysis must be based on a nonlinear motion of the wheelset on the track with random irregularities. Such a computer program was unavailable. Hence, the determination of the wear based on a limit cycle motion of the bogie (near to the critical speed) with different amplitudes is considered. The quasi-sinusoidal motion of the wheelset was calculated by Moelle's program[27]. An object of our project was to investigate the difference between calculating the wear rate from the exact nonelliptical contact area and the elliptical contact area. This comparison for the results of the quasi-sinusoidal motion with maximum amplitudes of 2.0 mm and 4.5 mm are represented in Fig. 11. It can be seen that:

- In both cases more material is removed from the wheel and rail in the boundary region of the motion curve than in central region of the motion curve. The quasi-sinusoidal motion and the jump of the contact point at 0.2 mm are responsible for this.
- The comparison of the results for nonelliptical contact areas and the elliptical contact areas indicates that despite the similar behaviour of the curves, the wear rates obtained in the two cases differ considerably, especially in the central region (see Fig. 11). This is a reflection of the fact that in this region, in the case of nonelliptical

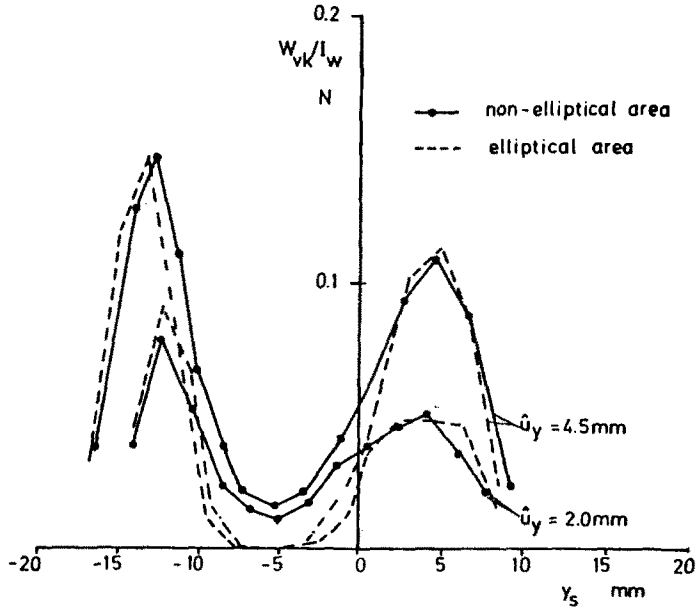

Fig. 11. Distribution of wear rate on track profile for elliptical and nonelliptical contact area.

contact areas, the wheel and rail come into contact more frequently than in the case of elliptical contact area. Hence, in order to obtain the real worn profiles of a combination of new wheel and rail profiles in which there is a jump of the contact point in the region near the central position, the nonelliptical contact areas should be used.

5. CONCLUDING REMARKS

The numerical method developed in the present study enables us to calculate the tangential stresses in the nonelliptical contact area between the two elastic bodies in rolling contact. The determination is based on Kalker's simplified nonlinear theory. To use this simplified theory, the coefficients of creepages must be known first. An approximate method is proposed to estimate these coefficients. A comparison shows that the approximate solutions for the tangential forces in the contact areas coincides excellently with those given by Kalker.

In the nonlinear determination of the tangential stresses and in the investigation of the subdivision of the contact area into a slip and an adhesion region, it is found that the slip area in a nonelliptical contact area deviates greatly from that in the Hertzian elliptical contact area. Wear occurs due to slip in parts of contact area and causes the change of wheel and rail profile, which in turn influences the conditions of lateral stability of railway vehicles. The first investigation represented the distribution of wear rate over rail profile considering both nonelliptical and elliptical contact areas. It is shown that cause of the quasi-sinusoidal motion of the wheelset against rail and the jump of the contact point near the central position of motion more material are removed at the boundaries of motion than those in central position of motion. This produces the actual wheel and rail profile which must be taken into account in next computation step of the investigation of running behaviour of the wheelset.

In addition to a limit cycle motion, the random motion caused by track irregularities must be taken into account. This is a next aim of our project. Thus, it will then be possible to calculate the long-term development of wheel and rail profiles.

Acknowledgements—The authors are grateful to Deutsche Forschungsgemeinschaft (DFG) for providing the financial support required to carry out this analysis and to the Computing Centre of Technical University of Berlin for the use of their facilities.

REFERENCES

1. H. Hertz, Über die Berührung fester elastischer Körper. *J. reine u. angew. Mathematik* **92**, pp. 156–171 (1982).
2. W. Hauschild, *Die Kinematik des Rad-Schiene-Sytems*. 2. Institut für Mechanik, TU Berlin (1977).
3. J. J. Kalker, On the rolling contact of two elastic bodies in the presence of dry friction. Diss. TH Delft. (1967).
4. F. W. Carter, On the action of a locomotive driving wheel. *Proc. Roy. Soc. London* **A112**, pp. 151–57 (1926).
5. H. Poritsky, Stresses and deflections of cylindrical bodies in contact with application to contact of gears and locomotive wheels. *J. Appl. Mech., Trans. Am. Soc. Mech. Eng.* **72**, S. 191–201, Discussion pp. 465–68 (1950).
6. F. Fromm, Berechnung des Schlupfes beim Rollen deformierbarer Scheiben. *ZAMM* **7**(1), pp. 27–58 (1927).
7. L. Föppl, *Die strenge Lösung für die rollende Reibung*. Leibniz-Verlag, München (1947).
8. H. Buffler, Beanspruchung und Schlupf beim Rollen elastischer Walzen. *Forsch. Ing.-Wes.* **27**(4), S. 121–26 (1961).
9. G. Heinrich and K. Desoyer, Rollreibung mit axialem Schub. *Ing.-Arch.* **36**, pp. 48–72 (1967).
10. K. L. Johnson, The effect of a tangential contact force upon the rolling motion of an elastic sphere on a plane. *J. Appl. Mech.* **25**, pp. 339–46 (1958).
11. D. J. Haines and E. Ollerton, Contact stress distribution on elliptical contact surfaces subjected to radial and tangential forces. *Proc. Inst. Mech. Eng.* **177**(4), S. 95–114 (1963).
12. J. J. Kalker, The computation of three dimensional rolling contact with dry friction. *Int. J. Num. Meth. Eng.* **14**, pp. 1293–1307 (1979).
13. J. J. Kalker, The contact between wheel and rail. Report of the Department of Mathematics and Informatics No. 82/27, TH Delft (1982).
14. K. Knothe and H. Le The, Ermittlung der Normalspannungsverteilung beim Kontakt von Rad und Schiene. *Forsch. Ing.-Wes.* **49**(3), pp. 79–85 (1983).

15. K. Knothe and H. Le The, A contribution to the calculation of the contact stress distribution between two elastic bodies of revolution with non-elliptical contact area. *Int. J. Comp. Struct.* **18,** pp. 1025–1033 (1984).
16. A. E. H. Love, *A Treatise on the Mathematical Theory of Elasticity*. 4th Ed. Cambridge UP (1926).
17. J. J. Kalker, Simplified theory of rolling contact. Delft Progress Report No. 1, S. 1–10 (1973).
18. J. J. Kalker, A fast algorithm for the simplified theory of rolling contact. Manuscript TH Delft (1980).
19. H. Le The, Normal- und Tangentialspannungsberechnung beim rollenden Kontakt für Rotationskörper mit nichtelliptischen Kontaktflächen. TU Berlin ILR-Mitt. Nr. 109 (1982).
20. J. J. Kalker, Transient phenomena in two elastic cylinders rolling over each other with dry friction. *J. Appl. Mech.* **37,** pp. 677–88 (1970).
21. R. Holm, *Electric Contracts*. Gebers Verlag. Stockholm (1947).
22. F. T. Burwell and C. D. Strang, Metallic wear. *Proc. Roy. Soc. London* **A212**(1111), pp. 470–77 (1952).
23. J. F. Archard, Contact and rubbing of flat surfaces. *J. Appl. Phys.* **24,** pp. 981–88 (1953).
24. J. F. Archard and W. Hirst, The wear of metals under unlubricated conditions. *Proc. Roy. Soc. London* **A238,** pp. 515–28 (1957).
25. I. V. Kragelski, *Grundlagen der Berechnung von Reibung und Verschleiß*. Carl Hanser Verag, München u. Wien (1983).
26. G. Fleischer, Energetische Methode der Bestimmung des Verschleißes. *Schmierungstechnik* **4**(9), pp. 269–74 (1973).
27. D. Moelle, Der Lauf eines Radsatzes unter vereinfachter Berüacksichtigung von Nichtlinearitäten. TU Berlin, ILR—Mitt. Nr. 88 (1981).